Comparisons of Multipath Modeling Strategies for the Estimation of GPS Positioning Error

Adrien Chen[1], Alexandre Chabory[2], Anne-Christine Escher[3], Christophe Macabiau[4]

ENAC

7 av Edouard Belin, BP 54005, 31055 Toulouse, France

1chen@recherche.enac.fr

2chabory@recherche.enac.fr

3escher@recherche.enac.fr

4macabiau@recherche.enac.fr

I. INTRODUCTION

For precise GPS positioning one major source of error is multipath. Therefore, it is important to get information about the possible multipath signals in a complex scenario such as urban or suburban man-made environments. We can distinguish three kinds of prediction models in the literature. Deterministic models, based on an electromagnetic description of multipath, require a precise description of the 3D receiver's environment in order to predict channel parameters [1]-[4]. Statistical models derive channel statistics by means of a statistical description of the environment based on extensive experimental data [5]-[6]. Finally, hybrid deterministic-statistic models are based on both deterministic techniques to simulate the basic characteristics of the channel and statistical add-ons [7]-[10]. The main interest of hybrid models is to achieve a realistic channel representation while maintaining an acceptable computation time in comparison to pure deterministic models. Here we focus on deterministic models. Most of them predict multipath by combining ray tracing techniques with geometrical optics (GO) or with the uniform theory of diffraction (UTD). Moreover, in these models the influence of small elements and material characteristics are generally not assessed in the simulation results.

In this article, we aim at two main objectives. The first objective is to propose a model based on physical optics (PO) in which field propagation is not approximated by rays, and to compare its performance with GO and UTD. The second objective is to specify a suitable description of the 3D environment (level of details and material characteristics) for multipath simulations.

In the next sections, we first introduce the GPS channel model, then we present GO, UTD and PO approaches. Finally simulations are performed to compare these approaches and to determine a suitable description of the environment.

II. PRESENTATION OF THE SIMULATION SOFTWARE

A. Channel Modeling

Between one satellite and the receiver, multipath corresponds to the fact that instead of receiving only the desired GPS signal, the antenna receives the aggregate of the direct signal and one or several reflected signals following indirect paths. If $x(t)$ represents the emitted waveform by a satellite, the received signal $y(t)$ is a sum of attenuated, time-delayed versions of $x(t)$. Here we use the classical impulse response function $h(t)$ for multipath channels given by [11]

$$h(t) = \sum_{k=1}^{K} a_k \delta(t - \tau_k) e^{j\phi_k}, \qquad (1)$$

with t the observation time, δ the Dirac distribution and K the number of multipath components. Further, (a_k, τ_k, ϕ_k) are the amplitude (or gain), arrival time and phase of the k-th path, respectively. For the sake of this paper they are assumed time invariant. Finally, the channel is entirely described by the parameters (a_k, τ_k, ϕ_k) for $k = 1...K$.

B. Principle of the Simulation

The principle of the complete simulator is illustrated in Fig. 1. The input parameters of the multipath generator are the satellite position, the receiver position, and the 3D modeling of the environment composed of planar dielectric and metallic facets. The role of the multipath generator is to predict the channel parameters. These parameters become the input of the GPS receiver simulator which returns the receiver position error.

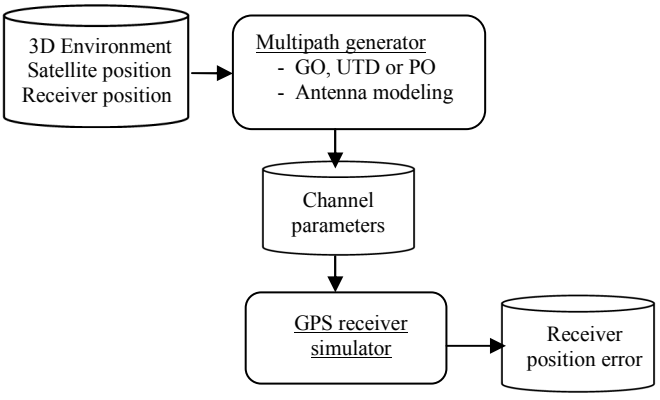

Fig. 1 Principle of the coupling between the multipath generator and the GPS receiver simulator

The multipath generator is composed of two main blocks. The first one predicts the list of the electromagnetic fields associated with each multipath. These fields can be computed either by GO, UTD or PO. The second one simulates the GPS receiver antenna. It allows the computation of the multipath parameters (a_k, τ_k, ϕ_k) from the electromagnetic fields via the use of the effective vectorial height of the antenna. In this paper we do not present the GPS receiver simulator developed by ENAC. Information about GPS receiver's settings can be found in [12].

C. Geometrical Optics

For GO and UTD predictions we use MUSICA, a full-wave prediction software developed by ENAC [12]. With GO, each multipath corresponds to a single ray between the satellite, a facet and the receiver which respects Fermat Principle. The direct signal reaching the antenna and one reflection on a facade are illustrated in Fig. 2. With UTD, rays associated with edge diffraction are added.

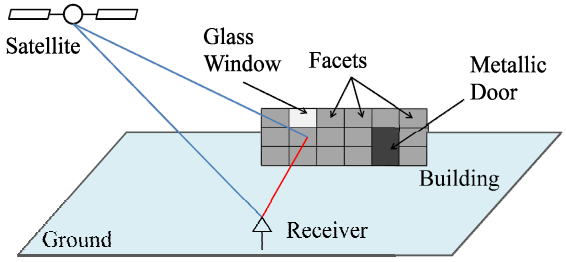

Fig. 2 Direct signal and one GO multipath due to a facade

D. Physical Optics

1) *Multipath Computation:* We propose an approach to predict multipath using PO. Within this approach, each illuminated surface generates reflected field. Since the environment is described by a set of facets, each illuminated facet is at the origin of one multipath as illustrated in Fig. 3.

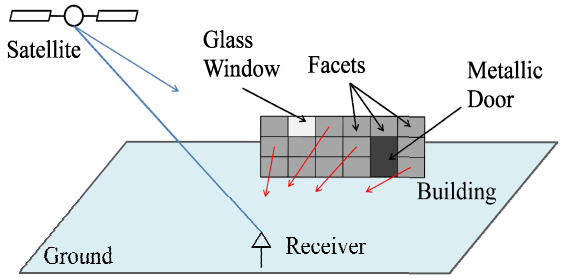

Fig. 3 Direct signal and several PO multipath due to a facade

Field amplitude and phase of each multipath are computed at the L1 frequency and delays correspond to the geometrical delays of the path satellite-facet-receiver. In order to reduce the computation time of the surface integral that appears for each facet with PO, we use the Mittra and Lee method described in [13]. This technique is only valid for receivers located in the far-field of each facet. Therefore, the facet size D must be chosen small enough so that the distance d between the receiver and the facets respects the condition

$$d > 2D^2/\lambda \tag{1}$$

with λ the signal wavelength.
Moreover, our PO approach takes into account double reflections between the facets and the ground assuming an infinite planar dielectric or metallic terrain.

2) *Multipath Reduction:* Since each illuminated facet generates a multipath, the computation load can become important in case of a complex 3D scene. In order to reduce the number of multipath we group adjacent multipath. If (a_1, τ_1, ϕ_1) and (a_2, τ_2, ϕ_2) are the characteristics of two multipath to be grouped, they are reduced as one equivalent multipath defined by

$$a = \left|a_1 e^{j\phi_1} + a_2 e^{j\phi_2}\right|, \tag{2}$$

$$\tau = \frac{a_1^2\tau_1 + a_2^2\tau_2}{a_1^2 + a_2^2}, \tag{3}$$

$$\phi = \arg\left(a_1 e^{j\phi_1} + a_2 e^{j\phi_2}\right). \tag{4}$$

In order to ensure the validity of this multipath reduction, a criterion on the delays, τ_1 and τ_2 has to be defined. In the frequency domain, the sum of the two initial multipath corresponds to

$$H(f) = a_1 e^{-j2\pi f\tau_1} e^{j\phi_1} + a_2 e^{-j2\pi f\tau_2} e^{j\phi_2}. \tag{5}$$

Note that at the central frequency, i.e. $f = 0$, we find back the equivalent values for a and ϕ. Introducing τ in (5), we deduce that H may be reduced to one multipath if the condition

$$a e^{j\phi} = a_1 e^{j\phi_1} e^{-j2\pi f(\tau_1 - \tau)} + a_2 e^{j\phi_2} e^{-j2\pi f(\tau_2 - \tau)} \tag{6}$$

is respected in the entire GPS band. This leads to

$$|\mathrm{B}(\tau_1 - \tau_2)| \ll 1, \tag{7}$$

where B is the bandwidth of the GPS L1 signal. Hence two multipath can be grouped only if their delays respect this condition.
Moreover, all the multipath with a delay such that

$$\tau > \frac{3}{2} T_C \tag{8}$$

are rejected since they do not have any influence on the GPS position [12]. The code period T_C is given by $1/F_C$ where F_C is the GPS L1 C/A code frequency ($F_C = 1.023Mhz$). Multipath delay of $3T_C/2$ corresponds to a delay distance of approximately 440m. In our application we consider this distance as the observation range limit, which means that objects further than 440m from the receiver antenna are neglected.

III. SIMULATIONS

A. Methods Comparison

1) *Configuration:* In this section, we focus on the multipath generator of our prediction model (Fig. 1). We compare the ability of GO, UTD and PO to produce accurate channel parameters in canonical configurations in order to determine the best modeling choice.

We consider two scenes. The first one is a large rectangular metallic reflector of size (69.6m x 16.2m), which corresponds to an ENAC campus building (Fig. 4). The second scene is a smaller metallic rectangular reflector of size (3.3m x 1.6m), which may correspond to a window of the preceding building. Reflectors are facetted in squares of side 0.5m. The antenna is modeled as isotropic, right-hand circularly polarized (RHCP) and with a polarization mismatch factor of –5dB. The incident field coming from the satellite is a RHCP plane wave, with an incidence of azimuth $\theta = 45°$ and elevation $\phi = 0°$. Using (2), (3) and (4), multipath of delays less than $10^{-3}.T_C$ are grouped.

2) *Large reflector:* In Fig. 5, we expose the Power Delay Profiles (PDP) $|h(t)|$ obtained with the different methods for a receiver located in front of the large metallic reflector.

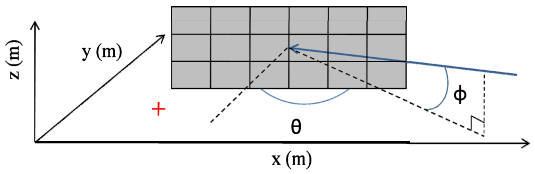

Fig. 4 Configuration of the simulations (the red dot represents the receiver position)

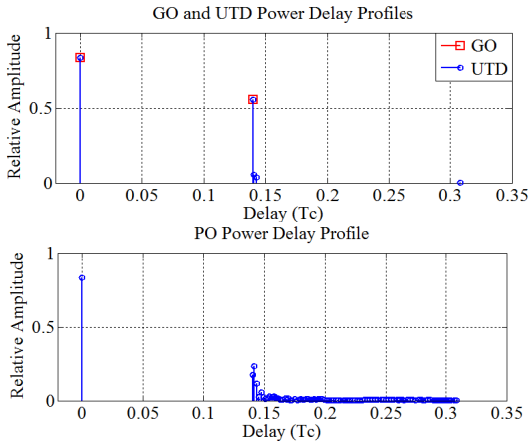

Fig. 5 Comparison of the GO, UTD and PO Power Delay Profiles

The UTD PDP highlights the presence of one direct path, followed by one reflected and 4 diffracted multipath. On the other hand, the PO reduced PDP (obtained after the multipath reduction process) shows one direct path followed by an important number of reflected multipath. Hence, it appears difficult to compare the PDPs of the channel models. To establish a comparison criterion, a more suitable way consists in looking at the results in the frequency domain. In Fig. 6, we observe the transfer functions obtained with PO, GO and UTD in the GPS frequency band. We denote that PO and UTD match, whereas slight differences exist if only GO is employed.

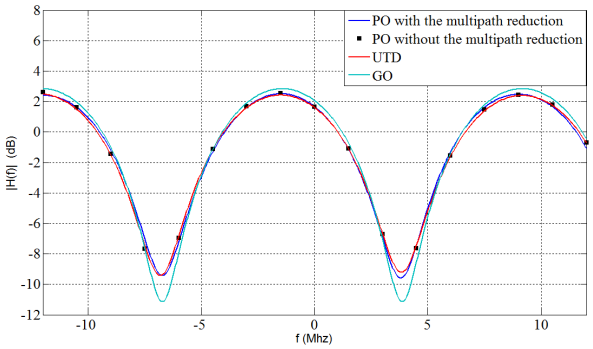

Fig. 6 Transfer functions of the GPS multipath channel using the different modeling approaches

Note also in this figure that the PO multipath reduction does not affect the PO channel transfer function. We define an average quadratic difference between 2 results $h_1(t)$ and $h_2(t)$ as

$$\epsilon_{mq} = \frac{\int_{-B/2}^{B/2} |S_{GPS_{L1}}.(H_1(f) - H_2(f))|^2 df}{\int_{-B}^{B} |S_{GPS_{L1}}|^2 df}, \qquad (9)$$

with $S_{GPS_{L1}}$ the spectrum envelop of the GPS L1 signal. From the receiver point of view, two models predicting the same transfer functions in the GPS band are strictly equivalent. We can consider that two predictions fit correctly if $\epsilon_{mq} \leq -20dB$.

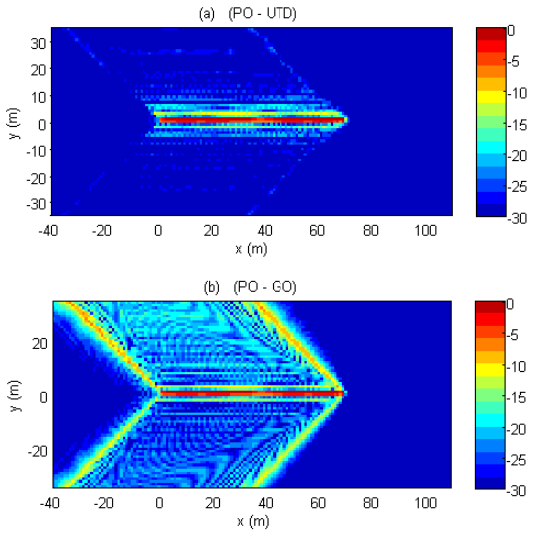

Fig. 7 Average quadratic difference between: (a) PO and UTD, (b) PO and GO

In Fig. 7 (a) we depict ϵ_{mq} in the vicinity of the reflector at a height of 8.1m. We notice that PO and UTD match except at distances below one meter from the reflector where ϵ_{mq} is about 0dB. These significant differences are due to the fact

that at this distance, we are not in the far-field of the facets as imposed by (1), thus PO is not valid. To reduce this error in PO, smaller facets can be employed, which will however yield longer computation times. Fig. 7 (b) shows large differences between GO and PO near the reflector, and also near the shadow boundaries where ϵ_{mq} can be of order -5dB. Hence, GO produces significant errors near the shadow boundaries.

3) *Small reflector:* We now focus on the case where the reflector is smaller. Fig. 8 illustrates the field on the axis of specular reflection.

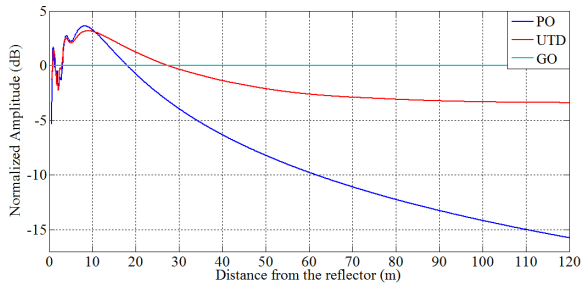

Fig. 8 Reflected electric field computed with PO, UTD and GO

In the far-field zone of the reflector, we observe significant differences in the methods. Indeed, only PO gives consistent results, i.e. a field that decreases in $1/r$ with r the distance from the reflector. UTD and GO results are non-physical because there are caustics in the pencil of reflected and diffracted rays [14]. Indeed, we consider an incident plane wave on a planar object, and we observe in the far-field zone of the reflector. Hence the UTD prediction only gives valid results in the near-field zone of the reflector i.e. approximately for

$$r < D^2/2\lambda. \qquad (10)$$

4) *Selection of the model:* In the GPS context, for large facades, the observation range of interest ($r \leq$440m) remains in the near-field zone of the object. In this configuration we have shown that UTD and PO gives similar results while differences exist with GO near the shadow boundaries. For small planar objects, the observation range of interest may reach the far-field zone of the object, inside which we have observed non-physical results with UTD and GO.

At the maximum observation distance ($r = 440\text{m}$), the minimal acceptable size of objects that GO and UTD can treat may be estimated using (10), which leads to a limit of about 13m.

In this paper, we want to consider complex scenes with objects of size few meters; therefore we choose to employ PO in the next section.

B. Choice of an Appropriate Description of the Environment

1) *Configuration and comparison criterion:* We now employ the complete prediction model of Fig. 1 in order to evaluate the influence of the environment description. Notice that the receiver range error is the determinant output when the complete simulator is analyzed.

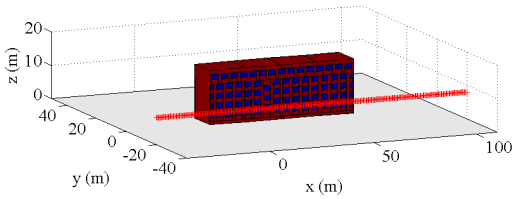

Fig. 9 Realistic 3D model of an ENAC building (the red dots stand for the receiver position)

As a realistic configuration, we consider a complete 3D model of the ENAC building (Fig. 9), described by means of dielectric multilayer facets. The building is made of concrete walls with glass windows. The ground is assumed to be asphalt. The satellite azimuth and elevation angles are 45° and 15°, respectively. In the receiver, the RF front-end filter bandwidth is set to 24Mhz, and the Early-minus-Late chip spacing [12] has a value of $0.25Tc$.

The total electric field at a height of 8.1m is depicted in Fig. 10.

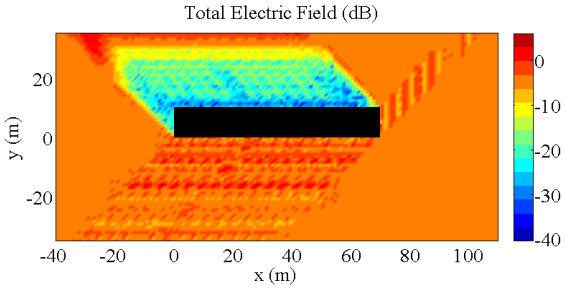

Fig. 10 Total electric field at a height of 8.1m

In the following simulations, we analyze the range error for a receiver located on a trajectory parallel to the x axis, at 20m from the building, and at a height of 8.1m (Fig. 9). This error is computed at each point for a static receiver and satellite.

2) *Influence of few-meters element:* First of all we want to assess the influence of details in the scene. Hence we perform simulations either with or without the windows in the 3D modeling. Fig. 11 illustrates the range error between the satellite and the receiver computed along the trajectory.

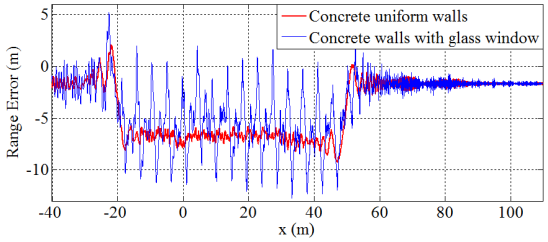

Fig. 11 GPS receiver estimated range error for concrete uniform walls and non uniform walls (with glass windows)

As could be expected there exists significant range error in the specular reflection zone ($-20m \leq x \leq 50m$). Outside this zone the residual error originates in the ground reflection.

The general behavior of the range error remains similar regardless the presence of windows. However, windows induce locally large oscillations of order of 10m.

3) *Influence of materials characteristics*: Next, we propose to assess the influence of the material characteristics. For this purpose we present simulations with different modeling parameters of the environment. Fig. 12 illustrates the receiver range error for hardened, reinforced and aerated concrete of permittivity $\varepsilon_r = 6.5 - j0.4$, $\varepsilon_r = 7 - j0.3$ and $\varepsilon_r = 2 - j0.5$, respectively [15].

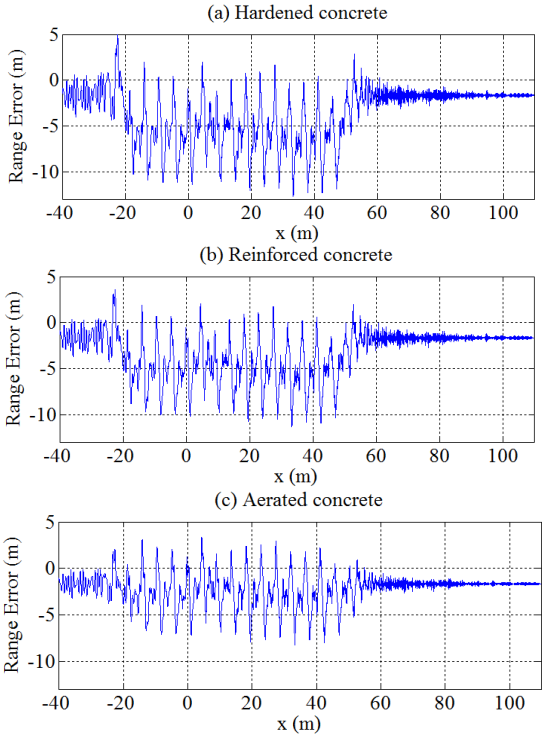

Fig. 12 GPS receiver estimated range error with concrete modeled as (a) hardened, (b) reinforced and (c) aerated

Hardened and reinforced concrete modeling present similar impact on the range error. However, these differences become significant when concrete is modeled as aerated. This result shows the importance of a precise knowledge of the building materials for the estimation of multipath error.

IV. Conclusions

In this article, two objectives were planned: the choice of an appropriate electromagnetic multipath model, and a suitable description of the environment.

To this end, we have developed a 3D prediction software based on PO to model the impact of multipath onto GPS positioning error. It accounts for the 3D environment, the presence of a flat dielectric terrain, the receiver antenna and the GPS receiver behavior.

Simulations performed with this tool have shown that PO and UTD prediction match whenever the observation range remains in the near field zone of the element. In the far-field zone of the element only PO yields physical results. In GPS context, the minimal acceptable size of objects that GO or UTD can treat may be estimated at approximately 13m. Besides, GO is inaccurate near the shadow boundaries.

Concerning the environment description, we have observed that small elements, e.g. doors and windows, may have a significant influence on the receiver range error. However, they can be precisely accounted only if their dielectric characteristics are precisely known, which might not be the case with building materials for instance.

For future work, a complementary statistical prediction could be added to account for the lack of knowledge of the environment.

Acknowledgment

The authors wish to thank Airbus for funding this work.

References

[1] R.Ercek, P. De Doncker and F. Grenez, “Study of pseudo-range error due to non-line-of-sight-multipath in urban canyons,” *in Proc. ION GNSS*, Sept. 2005.

[2] R.Ercek, P. De Doncker and F. Grenez, “Statistical determination of the pseudo-range error due to non-line-of-sight-multipath in urban canyons,” *in Proc. ION GNSS*, Sept. 2006.

[3] J. Legenne, J-J. De Ridder, “Performance of satellite navigation in urban areas with augmentations and hybridizations,” *in Proc. ENC GNSS*, Apr. 2003.

[4] HR. Anderson, “A ray-tracing propagation model for digital broadcast systems in urban areas,” *IEEE Trans. Broadcast*, vol. 39, no. 3, Sept. 1993.

[5] H. Suzuki, “A statistical model for urban radio propagation,” *IEEE Transactions on Communications*, vol. Com-25, no.7, Jul. 1977.

[6] G.L. Turin, F.D. Clapp, T.L. Johnston, S.B. Fine, “A statistical model of urban multipath propagation,” *IEEE Trans. on Vehicular Technology*, vol. VT-21, no. 1, Feb. 1972.

[7] A. Steingaß, A. Lehner, F. Pérez-Fontán, E. Kubista, M.J. Martín, B. Arbesser-Rastburg, "The high resolution aeronautical multipath navigation channel", *IEEE PLANS,* Apr. 2004.

[8] B. Roturier, B. Chateau, “A general model for the VHF aeronautical multipath propagation channel,” *in Proc. Aeronautical Mobile Communications Panel*, Working Group D, Jan. 1999.

[9] O. Esbri-Rodriguez, A. Konovaltsev, A. Hornbostel, “Modeling of the GNSS directional radio channel in urban areas based on synthetic environments,” *in Proc. ION NTM*, Jan. 2004.

[10] C.Oestges, S.R. Saunders, D. Vanhoenacker-Janvier, “Physical statistical modeling of the land mobile satellite channel based on ray tracing,” *IEEE Microwave Antennas Propagation*, vol. 146, no. 1, Feb. 1999.

[11] G.L Turin, “Communication though noisy, random multipath varying channels,” M. Eng. Thesis, Massachusetts Institute of Technology, USA, Jun. 1956.

[12] C. Macabiau, B. Roturier, E. Chatre, A.Renard, « Airport multipath simulation for sitting DGPS reference stations,” *in Proc. ION NTM*, Jan. 1999.

[13] S.W. Lee, R.M. Mittra, “Fourier transform of a polygonal shape and its application in electromagnetics,” *IEEE Trans. on Antennas and Propagation*, vol. AP-31, no.1, Jan. 1983.

[14] D. A. McNamara, C.W. I. Pistorius, J. A. G. Malherbe, “*Introduction To The Uniform Geometrical Theory Of Diffraction,* Norwood, MA: Artech House, 1990.

[15] S. Stavrou, S.R. Saunders, “Review of constitutive parameters of building materials”, *The Institute of Electrical Engineers*, 2003.